

HIGH LEVEL WASTE MELTING EXPERIMENT

Robert D. Klett

Sandia Laboratories, Albuquerque, New Mexico 87115

Presented at Waste Management 75

Tucson, Arizona

March 25, 1975

Abstract

An overview is given of the Deep Rock High Level Nuclear Waste Disposal Process (DRD) and the first medium scale demonstration test (DRD-1). The DRD process consists of placing solidified high-level waste (or mixtures of high and low-level waste), either uncontained or in expendable containers, in holes several kilometers deep which are drilled into bedrock. With the holes 0.3 to 3 m in diameter, the radioactive decay heat would melt and mix the waste and surrounding rock. After resolidification in 5 to 20 years, the waste/rock matrix would form a dilute, low surface area, low leachability solid plug permanently emplaced several kilometers below the earth's surface.

Progress to date in identifying and developing DRD technology has centered around the DRD-1 test. In this experiment, a waste simulant was electrically heated to 1320° C in a 1 m by 0.15 m diameter cavity in a block of dolerite rock. The presence of convection and mixing were confirmed and the thermal model of the test was verified. The leachability of the resolidified rock/simulant matrix was low, and the experiment hardware survived the test environment. A scale-up of this test should be possible. Although the DRD concept has not been proven feasible, progress to date indicates that further study is warranted.

Introduction

Nuclear reactors and other radiation sources either produce radioactive waste, have radioactive wastes as processing by-products, or become radioactive wastes after their useful lifetimes have ended. If reactors are to provide a significant amount of the world's energy, a method must be developed to permanently dispose of these wastes or to convert them to a useful or safe form. Although conversion is the most desirable alternative, it has not been shown to be technically feasible so we may have to rely on disposal for safe disposition of radioactive wastes. For a disposal process to be acceptable, it must meet the following criteria.

1. The waste must be permanently isolated from present and probable future areas of habitation or visitation, potentially useful mineral resources, the food chain, water supplies, and the air supply. This implies that it must be placed in a remote, stable media and be immobile unless it can only move to a more desirable area.

2. Because of the extremely long isolation period required, the disposal process must be maintenance free and not depend on political or social stability.
3. The disposal process must not require hazardous processing, transportation, or implementation.

Although larger quantities of low level waste are generated, the disposal of high level wastes are technically more difficult because of long-term high-level toxicity and the large quantities of heat generated early in the decay process. High level wastes are now being held in recoverable storage units in several different forms. A high level waste disposal process should accommodate these aged wastes in their present or modified forms as well as freshly generated wastes in forms consistent with existing processes and processes under development. Possible selective isotope extraction should also be considered.

A survey of high level waste disposal concepts conducted by Battelle, Pacific Northwest Laboratory shows that there are several alternatives which are potentially safe and which may have acceptably low environmental effects. However, none of these concepts have been developed sufficiently to show that one is superior to the others. Sandia Laboratories is currently conducting research and analysis on three of the more promising concepts: bedded salt, sea bed, and deep rock. These studies have a dual purpose: to select the best concept or concepts while making progress toward developing an operational disposal system at the earliest practical date. The Deep Rock Disposal (DRD) program is the topic of this paper.

The DRD Process

DRD is a permanent disposal concept for high level or combined high and low level radioactive wastes. Figure 1 shows the stages of the process. Holes approximately 0.3 to 3 meters in diameter are drilled several kilometers into competent bedrock or basement rock. Solidified radioactive waste, either uncontained or in expendable containers, is placed in the lower uncased section of the drill hole. Radioactive decay heat produced by the waste melts the waste, the surrounding rock, and containers if they are used. Natural convection currents mix the molten rock and waste. During the heating period, high vapor temperature volatiles that are released from the waste and rock would recondense on the lower part of the casing and other gases would be collected and processed at the top of the drill hole. As the size of the melt surface increases and the heating rate of the waste decays, a time is reached when conduction losses into the surrounding rock exceed the heat generated and the rock/waste matrix begins to resolidify. After complete resolidification (typically 5 to 20 years), the waste is diluted to less than 5% of its original concentration, it has low leachability and a low total surface area, and it is permanently implanted several kilometers below the earth's surface. After resolidification of the matrix, the top of the melt cavity can be sealed with a low melt temperature glass which would be

melted by the heat in the matrix and surrounding rock. After further cooling, the glass would resolidify and the remainder of the access tube would be filled with concrete or other suitable fill material.

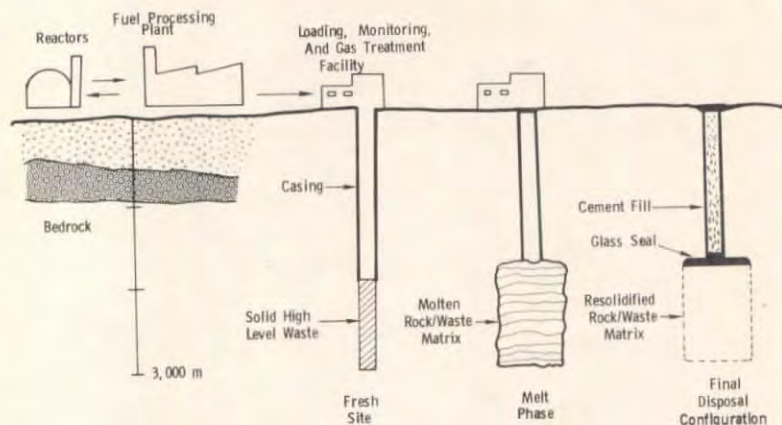


Fig. 1 Stages of Deep Rock Nuclear Wastes Disposal

In the long, thin cylindrical DRD configuration, the criterion that determines the extent of rock melting for waste of a given age is the initial power level per unit length of the cylinder. A power level of 20 kW/m at the time of burial is sufficient to melt enough rock to dilute 1 year old, high level waste by a factor of 25 or greater. This power level can be achieved by: (1) loading a small diameter hole with pure, young high level waste, (2) a larger diameter hole with aged high level waste, or (3) a large diameter hole with young high level waste mixed with old high level or any low level waste. The mixing could be accomplished by a radial and/or axial arrangement of old and young waste in their respective shipping containers as well as by uniformly mixed wastes. Table I lists several combinations that would produce an initial heating rate of 20 kW/m.

Table I

Waste Combinations That Produce 20 kW/m

Waste Form	Hole Diameter (m)
One Year Old High Level Waste	0.35
Five Year Old High Level Waste	0.80
Ten Year Old High Level Waste	1.13
Five Parts Low Level or Old High Level to One Part, One Year Old High Level Waste	0.88
Ten Parts Low Level or Old High Level to One Part, One Year Old High Level Waste	1.19

For a given initial heating rate per unit length, old waste will melt slightly more rock and will remain liquid longer than young waste mixtures. The CINDA digital heat transfer program, using temperature dependent material properties, was used to compute a typical melt cycle. It was assumed that a 1-meter diameter hole in an average bedrock was filled with 1-year-old waste diluted to 30 kW/m^3 . The decay rate was based on the curve for waste from a pressurized water reactor given in Reference 2. The melt radius history is given in Figure 2. The maximum melt radius is reached in 1.75 years, and the matrix is completely resolidified in 10.5 years. The maximum melt radius is 3.5 meters, corresponding to a waste dilution in the rock of approximately 50 to 1. Using approximate analytical methods, the centerline temperatures were computed to be less than 1500°C in this configuration.

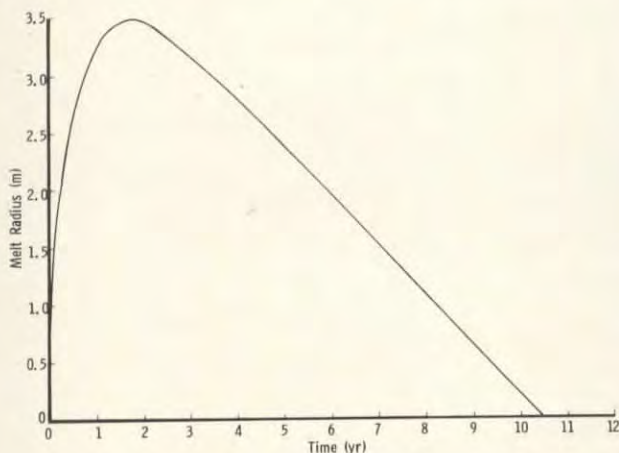


Fig. 2 Melt Radius for 30 kW/m^3 , 1-Year-Old Nuclear Waste Buried in a 1-meter Diameter Hole in an Average Bedrock

Capacities and drilling costs of a typical disposal site are given in Table II. The estimated total disposal costs of commercial high level waste, excluding transportation costs to the disposal site, are 0.004 mil/kWh electric.

Table II

High Level Waste Capacities and Costs of 1-m Diameter,
3000-m Deep Drill Hole with 1000 m of Waste Fill

Cost of 2/3 Cased Hole	\$4,200,000
Cost per m^3 Waste	\$5,400
Cost per kWh Electric	0.001 mil
Power Plant Capacity per Hole	390 GWe-yr
Holes per Year (Commercial Waste in Year 2000)	2.8

The DRD process includes several advantageous features. The many locations that are acceptable for DRD would eliminate or limit the transportation from the processing plants to the disposal site. No air or water transportation is needed unless DRD is used in conjunction with sea bed disposal. A stable disposal area could be selected that is far removed from habitation and mineral deposits. The melting of the waste and surrounding rock eliminates the need for active cooling, and isolation of the waste does not depend on the long term integrity of manmade containers. The final rock/waste matrix has a low leachability. The drill hole configuration with its large length to diameter ratio greatly reduces the vertical temperature gradient and hence should almost eliminate the upward migration of the circulating liquid. Because of the low concentration of waste (low total heat generation per unit length), the matrix is liquid for only a short period of time. This same feature limits thermal expansion stress and dislocation problems in the unmelted rock, and the fill hole provides space for expansion of the liquid. The small melt radius of the cylindrical configuration limits temperatures at the center of the melt and therefore limits volatilization of the melt. Various ages, forms, and concentrations of high level waste could be used in the DRD process; this would provide a means to dispose of old waste currently in storage, some low level waste, wastes that have had useful isotopes removed, and beneficial isotopes that have decayed below their useful level, as well as young solid high level waste. Solidified waste from a variety of processes could be used.

Although DRD appeared to be a promising process for the disposal of high level waste, there were numerous unanswered questions and potential engineering problems. Table III is a summary of the studies that will be needed to develop the process.

Table III
Research and Development Areas

1. Radionuclide Transport in Silicate Rock
 - Natural transport paths and mechanisms (e.g., underground water flow, seismic activity)
 - Matrix alteration caused by waste emplacement (e.g., thermal stress cracking, thermal degradation, chemical reactions, access holes)
 - Modes of transport (e.g., convection of molten material, solid diffusion, gas flow, water flow)
2. Thermal and Mechanical Processes
 - Convection in the melt
 - Temperature histories
 - Thermal expansion

3. Rock/Waste Matrix
 - Mixing
 - Solubility
 - Chemical reactions
 - Dehydration and gas generation
4. Hardware Development
 - Emplacement
 - Monitoring
 - Sealing
5. Cost and Environmental Impact

An analytical and experimental program is under way to evaluate the technical feasibility of DRD. Most of the progress to date has been derived from a medium scale rock and waste simulant melting experiment designated DRD-1.

The DRD-1 Test

The first step in developing DRD was to conduct an experiment that would demonstrate the concept, answer as many questions concerning the feasibility as possible, uncover potential problem areas, provide input data for analysis, and check the accuracy of analytical methods. The development of effective analytical models and representative testing methods is particularly important for waste disposal processes because these processes must be in remote locations which are difficult to monitor.

A schematic of the DRD-1 experiment is shown in Figure 3. The test was conducted in a 3 x 3 x 4.5 ft block of dolerite rock which was buried in granitic soil. The experiment was centrally heated with a 2.125-inch diameter silicon carbide heater with a 24-inch heating length. The heater was protected from the molten rock and waste simulant by a 3-inch diameter alumina tube covered with a platinum sheath. Semi-annular rings of a borosilicate glass waste simulant were loosely stacked in the 1-inch annulus around the tube. The waste simulant consisted of stable isotopes of representative waste or chemically similar elements. When the simulant melted, it filled the cavity to the top of the heating section. The cavity above the simulant was used to accommodate expansion of the rock as it changed from a crystalline solid to an amorphous liquid and the thermal expansion of the molten matrix.

Data acquisition during the test was accomplished with thermocouples, strain gages, sonic transducers, and a melt sampling pipet. There were 29 fixed thermocouples located in a radial and vertical array for ease in correlating with temperature gradients predicted analytically and to determine the effect of convection. There was

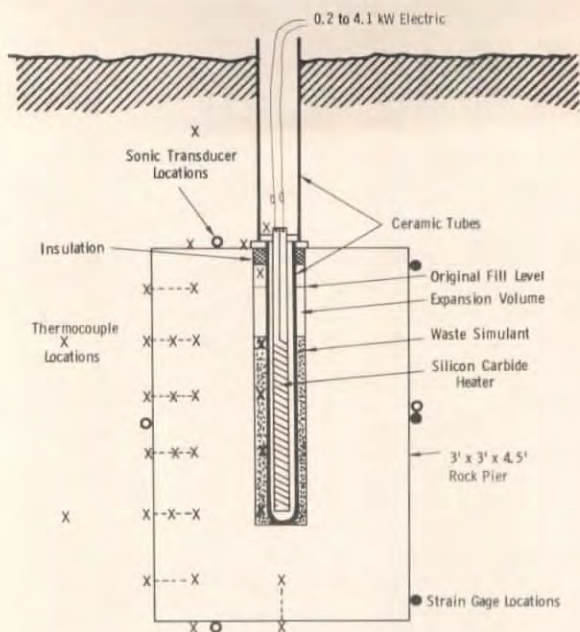


Fig. 3 Deep Rock Disposal Experiment 1

also a probe thermocouple that could be moved vertically in the melt which was used to obtain a continuous vertical temperature profile next to the heater tube and to locate the top of the liquid in the expansion volume. Three strain gages were located on the sides of the rock to check the surface strain predicted by the thermal stress analyses. Strain gage data were only good until the surface temperatures reached 350°F. Six ultrasonic LiNO_3 transducers were attached to the faces of the rock to locate any cracks that occurred during the test by using acoustic emission and triangulation techniques.

A pipet was used to extract samples of the melt to measure the amount of rock that had melted. The composition of the sample, and hence the ratio of rock to simulant, was determined by X-ray fluorescence spectroscopy. After the test, the rock was sectioned and one half was cut into smaller pieces for laboratory tests and analyses.

The heat pulse was a 43 day, 0.2 to 4.1 kW ramp followed by a 5 day hold at 4.1 kW. After the heat pulse, a small amount of power was supplied to the heater to assure cooling and solidification from the outer surface of the melt. Pretest temperature and thermal stress predictions were made using the CINDA and SAAS computer programs. The

mid section radial temperature predictions are shown in Figure 4. Vertical cracking due to thermal stresses was predicted based on limited high temperature mechanical property data. Details of the experiment and the test hardware can be found in Reference 3.

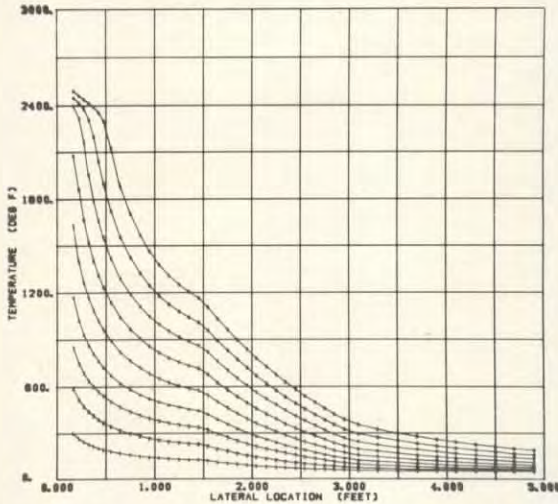


Fig. 4 DRD-1, Calculations Showing Low Viscosity in Melted Zone Data at 5, 10, 15, 20, 25, 30, 35, 40, 45 Days

Test Results

Temperature data from all the thermocouples were used to check the validity of the CINDA thermal model. Prior to melting, predictions were within a few percent of the data. However, near the end of the test, predictions were off by as much as 20%. This was due primarily to the vertical mass and energy transport caused by convection that cannot be handled in the current version of CINDA and to a lesser extent to inaccurate high temperature conductivity data.

Most of the test data concerning melting, expansion of the melt, mass transport, convection heat transfer, and rock cracking taken during the test were obtained by the probe thermocouple and the four thermocouples attached to the outer surface of the heater tube sheath (Nos. 3, 4, 5, and 6). At the beginning of the test when heat was transferred through the rock and simulant by conduction and across gaps by radiation and conduction, the temperatures of the top and bottom thermocouples (3 and 6) were lower than those of the middle thermocouples because heat was lost out the ends as well as radially (Figure 5). Number 3 had the lowest temperature because heat was also lost out the top by air convection in the expansion volume. Gap sizes around the solid simulant varied; hence, the thermal resistance also varied which accounts for the

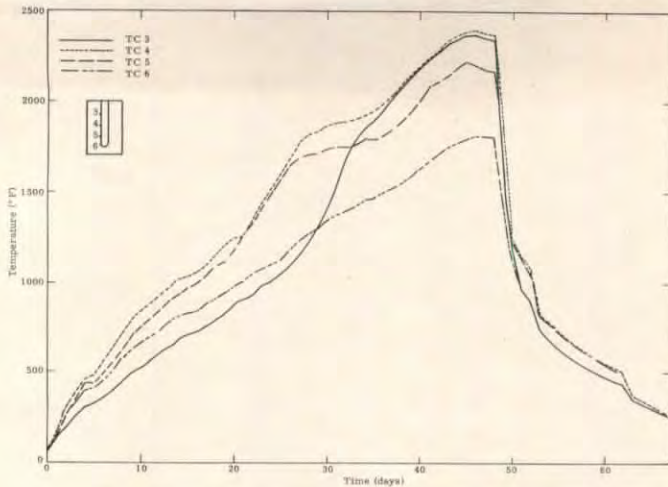


Fig. 5 Temperatures Along the Heater Tube

difference in the temperatures of Nos. 4 and 5. On day 21, the simulant began to soften and fill the gaps and the temperatures of Nos. 4 and 5 became nearly equal. The level of the top of the simulant also began to drop on day 21. Convection began at day 26 as indicated by a sharp rise in the temperature of No. 3 and a reduction in the slopes of Nos. 4 and 5 as heat was being transferred vertically by mass transport from the middle to the top. The slope of No. 6 began to decrease at about day 32 as the convection cell increased in size and nearly reached the bottom of the annulus. By day 37, the top of the rock had heated up and the vertical temperature gradient in the unmelted rock corresponded to the gradient in the circulating melt. At this point, a convection equilibrium was reached where the slopes of the four curves remained nearly constant, and the temperature changes closely followed changes in the heating rate.

The probe thermocouple was used to locate the top of the simulant, the top of the convection cell, and any solid materials that entered the annulus. With pure conduction heat transfer, the temperature would decrease in the upward direction in the top half of the rock. However, the upward temperature gradient is positive in the convection cell because of mass transport. Therefore, the top of the convection cell was located at the inflection point in Figure 6. On the 38th day of the test, the top part of the rock cracked, allowing a small amount of sand to run into the expansion volume. When the relatively cool sand contacted the surface of the viscous liquid, there was a small region of mixing which caused a crust to form between the sand and the molten matrix. The crust was soft enough to penetrate with the probe thermocouple.

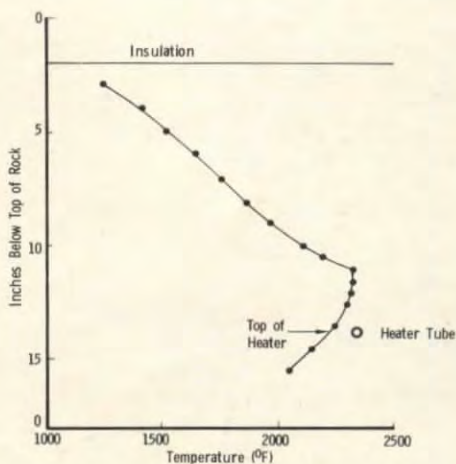


Fig. 6 Probe Thermocouple Temperatures, Day 45

The uncovered rock (Figure 7) showed vertical cracks as predicted by the SAAS computer program. The cracks were widest at the top, and only one extended to the bottom of the rock. The other three formed inverted T's or Y's about half way down. This pattern was probably caused by the large temperature gradients produced shortly after convection was established. Sonic transducers also indicated cracking on the 38th day of the test. This crack pattern in the relatively small parallelepiped containing a single convection cell is not indicative of cracking in an operational configuration in a much larger rock formation with a larger L/D ratio and multiple cells or turbulent flow.



Fig. 7 Post Test Crack Pattern

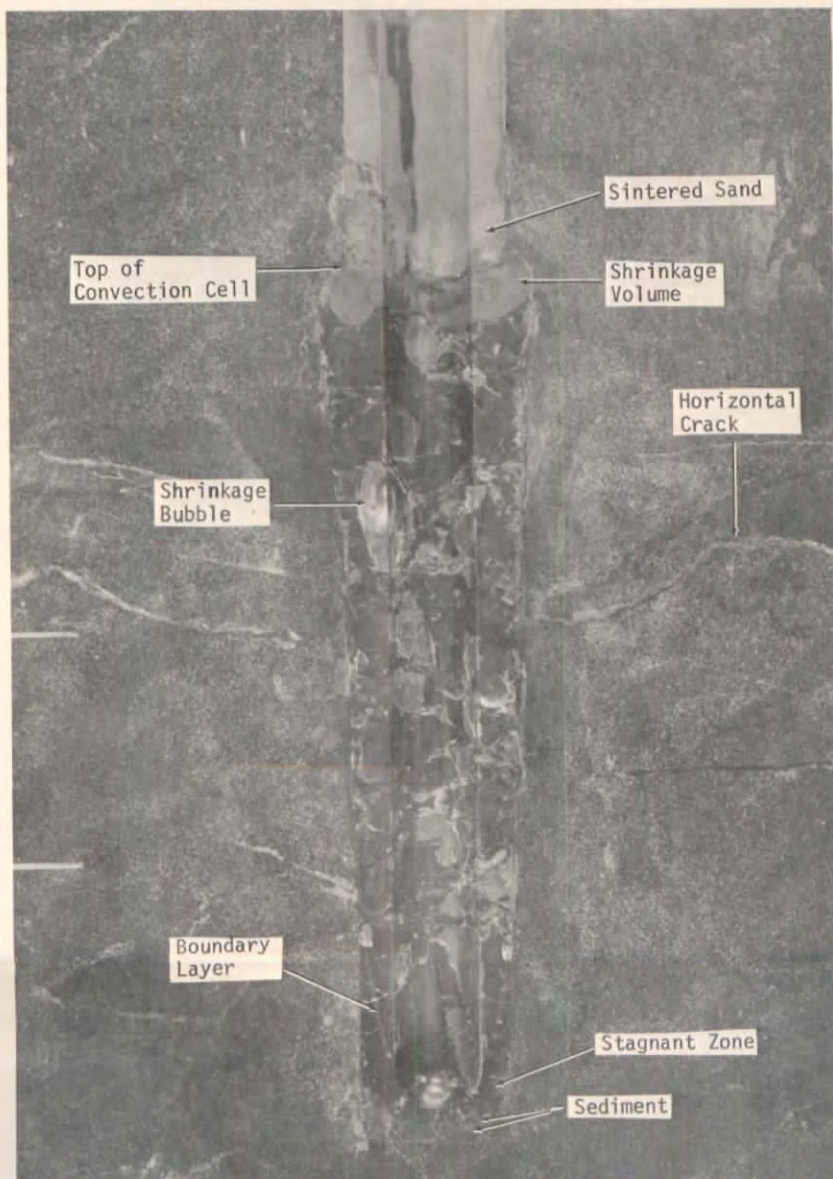


Fig. 8 Cross Section of the Rock/Simulant Matrix

Figure 8 shows a posttest vertical cross sectional view of the melt zone and surrounding rock with the heater tube removed. The melt diameter is 7.2 inches at the top. The discolored region out to about 8 inches from the melt is thermal degradation of the unmelted rock. Several horizontal thermal stress cracks appear near the middle of the rock. The matrix shrunk approximately 5% during resolidification. Most of the shrinkage volume appears at the top of the matrix, but a large bubble also formed about 7 inches from the top after the top of the matrix cooled and became immobile. There are numerous cracks in the rock/simulant matrix that formed during the rapid cooling of the experiment. This cracking should be reduced in an operational configuration that resolidifies over a period of years. The lower level of sand that ran into the expansion cavity sintered and remained in place after sectioning. The convection cell extended from the bottom of the sand to about 3 inches from the bottom of the melt. Near the bottom, the convection cell narrowed and is outlined by a light colored boundary layer. No rock melted below the point where the boundary layer separated from the rock/melt interface. A cross section view of the boundary layer separation at the wall is shown in Figure 9. The light irregular line is the edge of the convection cell. The bottom inch of the stagnant zone consists of a red and a brown layer of sediment. Figure 10 shows a horizontal cross section near the top of the matrix. Circulating melt enlarged the inner part of the cracks, but none of the melt penetrated more than 1.4 inches into the cracks. The cooler rock solidified the melt, forming a glassy seal. Several cooling cracks are also shown in Figure 10.



Fig. 9 Horizontal Cross Section Near the Bottom
of the Convection Cell



Fig. 10 Horizontal Cross Section Near the Top of the Matrix

The chemical analysis of the matrix that has been completed to date was conducted using X-ray fluorescence spectroscopy. Four distinct homogeneous zones were found, the large convection cell at the top and three stagnant zones near the bottom. A summary of the test results is shown in Figure 11. There was some segregation of elements from both the simulant and rock. The simulant percents shown are based on only six elements and do not indicate that any of the other simulant elements are present in the same concentrations. The compositions of the convection cell and upper stagnant zone, which make up 98% of the total volume, are nearly the same. The only stratification appeared in the lower 2% of the matrix. Since the elements that settled in DRD-1 would be generating heat in an operational disposal site, it is possible that they would remain in the convection cells. The other possibility is that separate convection cells containing

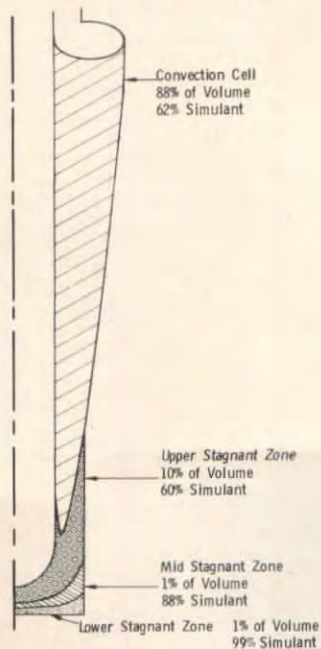


Fig. 11 Composition of Rock/Simulant Matrix Based on Ce, U, Sr, Y, Zr, and Mo

heavier molecules would form at the bottom of the melt. An electron microprobe analysis is under way to define the composition of crystals that formed during cooling and of the matrix glass in each of the four zones.

Leach experiments were performed on samples from each of the zones. The IAEA standard leach test procedure was used on both powder and bulk samples. The average leach rates of the matrix were lower than the waste simulant by a factor of 11 in the powdered form and a factor of 18 with the bulk samples. However, leach rates were still slightly higher than the best BNW borosilicate glass. Leach rates were lower in the top 98% of the matrix than in the sediment zones. It is not known if this difference is caused by different chemical compositions or by different crystal structures associated with different cooling rates. The effects of dilution and rock composition on the leachability of various waste forms must also be determined.

Thin section optical microscopy analyses were made of the melt zone and surrounding rock. A section of unaltered rock is compared to a section at the melt boundary in Figure 12. The feldspar (white) shows no signs of change prior to melting, but the mafic materials (gray) are oxidized 9 cm out from the melt as shown by a darkening of these minerals. There is a sharp melt front, with the mafic minerals melting slightly ahead of the feldspar. Voids observed on a cut surface within 1 cm of the melt boundary were the result of a mafic melt that was forced out, possibly by gas pressure. Voids observed farther than 1 cm from the melt were caused by the plucking of weak oxidized mafic grains from the surface during sample preparation. The dark shading in the melt near the boundary is caused by pyroxene and spinel crystalites which formed during the cooling process. The same small crystal formations are found in the light colored layer at the edge of the convection cell near the bottom of the matrix.

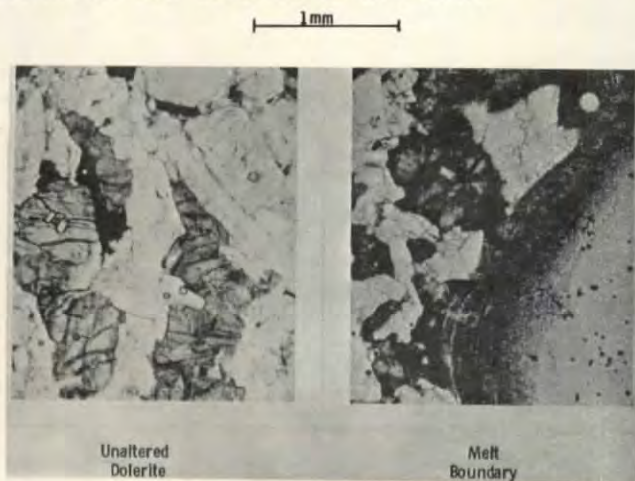


Fig. 12 Thermal Degradation of Dolerite

In the middle 13 inches of the matrix that was the last to resolidify, there were clusters of crystals that were formed from the supercooled state (Figure 13). Figure 14 is a reflected light micro-photo of one of these clusters. The rhombic shaped crystals are Mg-Fe spinels, and the swallow tail crystals are probably borates. Some of the spinels are made up of alternate layers of MgO and Fe₂O₃ rich materials, indicating that they were formed as they moved between hotter and cooler regions. This is another indication of convection currents even during cool-down.



Fig. 13 Crystal Clusters Near the Center of the Matrix

0.1 mm
┌───┐



Fig. 14 Thin Section Micrograph of a Crystal Cluster

Conclusions

Although the feasibility of the DRD process has not been proven, tests and analysis indicate that the concept deserves further study. Several minor changes in the concept have been made since its inception, but no major engineering obstacles have been found. Thermal stress and heat transfer analytical models have been adequate but they must be upgraded to handle convection, and more complete material properties are needed. The DRD-1 test was successful, and all test hardware survived. A scale-up of this type of experiment should be possible. Some of the data, technology, and analytical techniques from the DRD program are applicable to other geologic or related disposal concepts.

References

1. K. J. Schneider and A. M. Platt, "Advanced Waste Management Studies, High Level Radioactive Waste Disposal Alternatives," USAEC Report BNWL-1900, May 1974.
2. J. A. Angelo, Jr., and R. G. Post, "Nuclear Fuel Cycle and the Isotopic Compositions," Nuclear Technology, December 1974.
3. R. D. Klett, "Deep Rock Nuclear Waste Disposal Test: Design and Operation," SAND 74-0042, September 1974.

Acknowledgments

The author wishes to express his appreciation to those who contributed to the success of the DRD-1 experiment.

H. B. Austin, J. A. Barber, A. G. Beattie, E. K. Beauchamp, B. M. Brake, W. F. Chambers, F. C. Dain, R. J. Eagan, J. H. Gieske, E. J. Graeber, H. J. Gregory, K. Keil, B. T. Kenna, P. L. Nelson, H. Planner, R. H. Richards, J. T. Schamaun, F. V. Stohl, and A. C. Zuppero.

This work was supported by the United States Atomic Energy Commission.